Modal Representation of the Resonant Body within a Finite Difference Framework for Simulation of String Instruments

Orr, S., & Van Walstijn, M. (2009). *Modal Representation of the Resonant Body within a Finite Difference Framework for Simulation of String Instruments*. 213-220. Paper presented at Proc. 12th Int. Conference on Digital Audio Effects (DAFx-09), Como, Italy.

Document Version:
Peer reviewed version

Queen's University Belfast - Research Portal:
Link to publication record in Queen's University Belfast Research Portal

General rights
Copyright for the publications made accessible via the Queen's University Belfast Research Portal is retained by the author(s) and / or other copyright owners and it is a condition of accessing these publications that users recognise and abide by the legal requirements associated with these rights.

Take down policy
The Research Portal is Queen's institutional repository that provides access to Queen's research output. Every effort has been made to ensure that content in the Research Portal does not infringe any person's rights, or applicable UK laws. If you discover content in the Research Portal that you believe breaches copyright or violates any law, please contact openaccess@qub.ac.uk.

Open Access
This research has been made openly available by Queen's academics and its Open Research team. We would love to hear how access to this research benefits you. – Share your feedback with us: http://go.qub.ac.uk/oa-feedback

Download date:18. May. 2024

MODAL REPRESENTATION OF THE RESONANT BODY WITHIN A FINITE DIFFERENCE FRAMEWORK FOR SIMULATION OF STRING INSTRUMENTS

Sarah Orr and Maarten van Walstijn

Sonic Arts Research Centre - School of Electronics, Electrical Engineering and Computer Science
Queen's University Belfast
{sorr20,m.vanwalstijn}@qub.ac.uk

ABSTRACT

This paper investigates numerical simulation of a string coupled transversely to a resonant body. Starting from a complete finite difference formulation, a second model is derived in which the body is represented in modal form. The main advantage of this hybrid form is that the body model is scalable, i.e. the computational complexity can be adjusted to the available processing power. Numerical results are calculated and discussed for simplified models in the form of string-string coupling and string-plate coupling.

1. INTRODUCTION

Musical string instruments invariably comprise of a resonant body that is driven by forces that result from exciting strings that are coupled to the body. In sound synthesis applications, the string-body coupling is often simplified to a source-filter model, relying on the assumption that the impedance presented by the body to the string is much larger than the characteristic impedance of the string. While this assumption is reasonable for most practical cases, such models are not truely predictive. For instance, when modelling a body excited by more than one string polarity, there is no way of knowing how to calculate the sound radiating from the instrument, as the levels of contribution depend on the level of coupling at the bridge/body for each polarity. This is not necessarily a problem if the objective is to model a fixed instrument, as these levels can be fine-tuned empirically to give the certain desired sound (see, for example, the piano tone synthesis in [1]). The source-filter approach does however effectively shield the user from the fundamental design of the instrument, allowing flexibility only regarding the playing control of the instrument.

The long term aim of the authors of this paper is to develop physical models that allow user flexibility in both the design and the control of the instrument. This requires a more rigorous modelling approach, and immediately makes modelling the coupling between string and body and/or other elements such as a bridge one of the key challenges. Among the existing physical modelling paradigms, the finite difference (FD) method lends itself extremely well to rigorous modelling, because it directly simulates the equations that govern the physics of the instrument. With regard to modelling strings and their excitation, this means that there is no fundamental limitation with respect to incorporating nonlinear phenomena. More specifically, the FD method can be employed for rigorous modelling of geometric nonlinearities, i.e. spatially distributed non-linear coupling between the transverse and the longitudal polarisations of the string [2]. Most other paradigms, such as the Digital Waveguides (DW) [3] or the Functional Transformation Method (FTM) [4, 5], are fundamentally more limited in that regard, allowing only for simulation of tension modulation.

The FD method also has its disadvantages though, in particular it requires one to deal with numerical dispersion and numerical stability. The dispersion can usually be reduced significantly by designing compact implicit schemes. Stability analysis is straightforward for linear systems, for example by using the von Neuman method [6]. For non-linear systems however, energy methods are needed [2], and the process of designing appropriate schemes is somewhat less standardised, often presenting further challenges with regard to efficiency. One feature inherent to any FD model is that it cannot be scaled in terms of computational complexity without detrimental effects to the resulting output sound. That is, one may reduce the sample rate in order to scale down the processing and memory requirements, but besides the obvious consequence of a reduced model bandwidth, this invariably also means that the numerical artfecacts (dispersion, attenuation) inherent to the FD scheme used are more pronounced in lower frequency ranges. This contrasts with approaches that lead to a modal representation, such as the FTM, that render models that allow increasing efficiency by removing individual modes and/or by applying multi-rate processing methods [7]. This advantage can be particularly prominent for simulation of linear 2D or 3D systems, for which the numerical artefacts tend to be large in FD models, and the need for scalability high.

Given the desirability for the string model to be extendable to geometric nonlinearities, while the body may be assumed to behave linear, it is of interest to explore whether it is possible to model the string with the FD method while representing the body in a modal fashion, thereby getting the best of both worlds. The main challenge involved is how to numerically formulate the interaction between the string and the body. In this paper, we begin to address this question by considering a simplified string instrument in the form of a (linear) stiff string coupled transversely (with one end[1]) to a simply supported rectangular plate.

The general question of interfacing different physical modelling paradigms has been explored extensively recently [8, 9]. Among the main outcomes are two different interaction topology platforms, the BlockCompiler (BC) and the Binary Connection Tree (BCT) [9], that offer robust and flexible implementation by exploiting certain advantages of wave-domain connection units. It appears however that the specific case of directly connecting an FD model to a modal system has not been addressed yet in the literature.

The paper is laid out as follows. The main continuous-domain equations are given in section 2. In section 3, a full finite dif-

[1] The connection of the string end to a resonant body is directly applicable to, for example, harps, but is indirectly also useful as a model for instruments in which the string couples to the body via a bridge located away from the string ends.

ference model of a string coupled to a plate (the FD-FD model) is presented. This is followed by the FD-Modal formulation, in which the plate is represented in modal form, in section 4. Results generated with these models at 44.1 kHz are discussed in section 5, and concluding remarks are given in section 6.

2. A STRING COUPLED TO A RESONANT BODY

2.1. Transverse Vibrations of a String

Transverse vibrations of a stiff, lossy string can modelled using the following equation of motion [10]:

$$u_{tt} = c_u^2 u_{xx} - \kappa_u^2 u_{xxxx} - 2b_{1u}u_t + 2b_{2u}u_{xxt} + \rho_u^{-1}\mathcal{F}_u, \quad (1)$$

where t and x denote time and position along the string, respectively, and where using these as subscripts denotes partial differentiation, i.e.

$$u_t \equiv \frac{\partial u}{\partial t}, \quad u_x \equiv \frac{\partial u}{\partial x}, \quad u_{tt} \equiv \frac{\partial^2 u}{\partial t^2}, \quad u_{xx} \equiv \frac{\partial^2 u}{\partial x^2}. \quad (2)$$

The first two terms from the left in (1), in the absence of the others, will give rise to the wave equation for the ideal string. The parameter κ_u is related to stiffness and b_{1u} and b_{2u} denote a frequency-independent and frequency-dependent loss parameter, respectively. $\mathcal{F}_u$ is the force density (N/m) acting on the string and ρ_u is the mass density (kg/m) of the string. Applying a simply supported boundary condition at one of the ends of the string amounts to setting both the displacement and the bending moment to zero [11]. For example, at the left end of the string we have

$$u(0,t) = u_{xx}(0,t) = 0. \quad (3)$$

2.2. Transverse Vibrations of a Thin Plate

We aim to simulate the string coupled to a thin plate of homogeneous isotropic material, the vibrational character of which is dominated by stiffness [11]. If losses are included, the following equation can be used:

$$v_{tt} = -\kappa_v^2 \triangle^2 v - 2b_{1v}v_t + 2b_{2v}\triangle v_t + \rho_v^{-1}\mathcal{F}_v, \quad (4)$$

where $\triangle = (u_{xx} + u_{yy})$ and (x, y) are the spatial coordinates. Various boundary conditions are applicable here (i.e. free, clamped, simply supported). It is well known that only in the case of simply supported boundary conditions, the modes of the plate can be calculated analytically [11].

2.3. Coupling Conditions

Consider that the string is of length L and that its right end is rigidly coupled to the plate at a point (x_c, y_c). For a stiff string, the force that the string then exerts on the plate comprises of a tension term and a shear force:

$$F_c = -T_u u_x(L,t) + \kappa_u^2 \rho_u u_{xxx}(L,t). \quad (5)$$

The other conditions for rigid coupling are that the displacements of the string and plate are equal at the connection point, and that the bending moment of the string vanishes there (i.e. it cannot be transferred through the connection):

$$u(L,t) = v(x_c, y_c, t), \quad (6)$$
$$u_{xx}(L,t) = 0. \quad (7)$$

3. FD-FD FORMULATION

3.1. FD Formulation of the String

To solve equation (1), it may be approximated over a grid spacing X_u and time step T, with the difference operators defined as:

$$\delta_x \equiv \frac{u_{k+1}^n - u_{k-1}^n}{2X_u}, \quad (8)$$
$$\delta_t \equiv \frac{u_k^{n+1} - u_k^{n-1}}{2T}, \quad (9)$$
$$\delta_x^2 \equiv \frac{u_{k+1}^n - 2u_k^n + u_{k-1}^n}{X_u^2}, \quad (10)$$
$$\delta_t^2 \equiv \frac{u_k^{n+1} - 2u_k^n + u_k^{n-1}}{T^2}, \quad (11)$$
$$\delta_{t,-} \equiv \frac{u_k^n - u_k^{n-1}}{T}. \quad (12)$$

These operators can be applied to equation (1) as follows

$$\delta_t^2 u = -\kappa_u^2 \delta_x^2 \delta_x^2 u + c_u^2 \delta_x^2 u - 2b_{1u}\delta_t u + 2b_{2u}\delta_x^2 \delta_{-t} u + \rho_u^{-1}\mathcal{F}_u, \quad (13)$$

where the non-centered operator ($\delta_{t,-}$) is employed in order to avoid implicitness [10]. The final update equation[2] takes the form:

$$u_k^{n+1} = a_{1u}u_k^n + a_{2u}(u_{k+1}^n + u_{k-1}^n) + a_{3u}(u_{k+2}^n + u_{k-2}^n) + a_{4u}u_k^{n-1} + a_{5u}(u_{k+1}^{n-1} + u_{k-1}^{n-1}) + a_6\mathcal{F}_k^n, \quad (14)$$

and the Courant-Friedrichs-Lewy (CFL) condition of this scheme is:

$$X_u^2 \geq \tfrac{1}{2}c_u^2 T^2 + 2b_{2u}T + \sqrt{\left(\tfrac{1}{2}c_u^2 T^2 + 2b_{2u}T\right)^2 + 4\kappa_u^2 T^2}. \quad (15)$$

3.2. FD Formulation of the Thin Plate

The discretisation of (4) is carried out using an interpolated scheme adapted from [12], using the following approximation to the Laplacian:

$$\triangle \approx \hat{\triangle} = \alpha\delta_+^2 + (1-\alpha)\delta_\times^2, \quad (16)$$

with

$$\delta_+^2 = \delta_x^2 + \delta_y^2, \quad (17)$$
$$\delta_\times^2 = \delta_x^2 + \delta_y^2 + \frac{X_v^2}{2}\delta_x^2\delta_y^2, \quad (18)$$

where X_v is the spatial step in both directions (x, y), and where α is a free interpolation parameter ($0 \leq \alpha \leq 1$). It follows then that

$$\hat{\triangle}^2 = \alpha^2\delta_+^2\delta_+^2 + (1-\alpha)^2\delta_\times^2\delta_\times^2 + 2\alpha(1-\alpha)\delta_+^2\delta_\times^2. \quad (19)$$

Applying the difference operators to equation (4) yields:

$$\delta_t^2 v = -\kappa_v^2 \hat{\triangle}^2 v - 2b_{1v}\delta_t v + 2b_{2v}\delta_t \hat{\triangle} v, \quad (20)$$

[2] See appendix for all difference equation coefficient formulae.

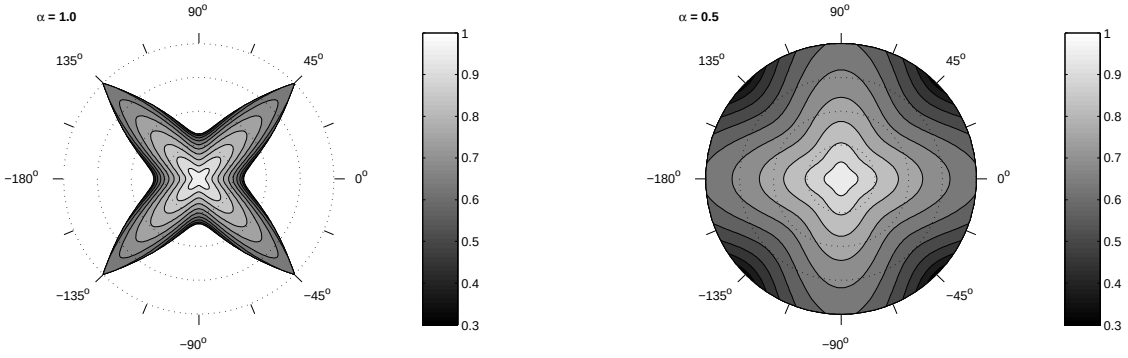

Figure 1: *Relative phase velocity of the FD plate formulation as a function of frequency (polar plot radius) and propagation angle (polar plot angle), for $\alpha = 1$ and $\alpha = 0.5$. In the plots, starting from the most inner circle, the dotted-line circles indicate $f = (\frac{1}{8}, \frac{1}{4}, \frac{3}{8}, \frac{1}{2})f_s$.*

and the final update equation becomes:

$$\begin{aligned} v_{l,m}^{n+1} &= a_{1v} v_{l,m}^n \\ &+ a_{2v}\left(v_{l+1,m}^n + v_{l-1,m}^n + v_{l,m+1}^n + v_{l,m-1}^n\right) \\ &+ a_{3v}\left(v_{l+1,m+1}^n + v_{l+1,m-1}^n + v_{l-1,m+1}^n + v_{l-1,m-1}^n\right) \\ &+ a_{4v}\left(v_{l+2,m}^n + v_{l-2,m}^n + v_{l,m+2}^n + v_{l,m-2}^n\right) \\ &+ a_{5v}\big(v_{l+2,m+1}^n + v_{l+2,m-1}^n + v_{l+1,m+2}^n + v_{l+1,m-2}^n \\ &\ldots \quad + v_{l-2,m+1}^n + v_{l-2,m-1}^n + v_{l-1,m+2}^n + v_{l-1,m-2}^n\big) \\ &+ a_{6v}\left(v_{l+2,m+2}^n + v_{l-2,m+2}^n + v_{l+2,m-2}^n + v_{l-2,m-2}^n\right) \\ &+ a_{7v} v_{l,m}^{n-1} \\ &+ a_{8v}\left(v_{l+1,m}^{n-1} + v_{l-1,m}^{n-1} + v_{l,m+1}^{n-1} + v_{l,m-1}^{n-1}\right) \\ &+ a_{9v}\left(v_{l+1,m+1}^{n-1} + v_{l+1,m-1}^{n-1} + v_{l-1,m+1}^{n-1} + v_{l-1,m-1}^{n-1}\right) \\ &+ a_{10v}\mathcal{F}_{l,m}^n. \end{aligned} \quad (21)$$

The CFL condition of this scheme is:

$$X_v^2 \geq 2T\left(b_{2v} + \sqrt{b_{2v}^2 + \kappa_v^2}\right) \cdot \max(1, 2\alpha). \quad (22)$$

In our example applications, we used $\alpha = 0.5$, which leads to the best possible scheme within the family of interpolated schemes, in that the numerical cut-off then lies at or near Nyquist for all propagation directions. Figure 1 illustrates the relative phase velocity of the scheme (the ratio between the discrete and the continuous wave velocity [12]) as a function of frequency and direction for $\alpha = 0.5$ as well as for the standard case of directly applying centered operators (i.e. $\alpha = 1$). The relative phase velocity data was calculated only for real wavenumbers, hence the edges of the plot indicate the numerical cut-off frequency, above which the wavenumbers become complex-valued (see [13] for a more detailed explanation of this type of plot).

3.3. Updating the Connection Point

For a string rigidly coupled to a plate, a special update equation has to be found for the connection point ($k = L/X_u$). Applying centered difference operators to equation (5) gives

$$F_k^n = -\frac{T_u}{2X_u}(u_{k+1}^n - u_{k-1}^n) + \frac{\kappa_u^2}{2X_u^3}(u_{k+2}^n - 2u_{k+1}^n + 2u_{k-1}^n - u_{k-2}^n), \quad (23)$$

Since u_{k+2}^n and u_{k+1}^n are so-called 'ghost points', i.e. they lie outside the bounds of the string, they must be eliminated from (23). Using equation (7) it can be shown that $u_{k+1}^n = 2u_k^n - u_{k-1}^n$. The ghost point u_{k+1}^n can therefore be substituted by $2u_k^n - u_{m-1}^n$. Writing (14) in terms of u_{k+2}^n and substituting for u_{k+1}^n, u_{k+2}^n in (23) yields:

$$\begin{aligned} F_c^n &= \theta\Big\{d_1 u_k^n + d_2 u_{k-1}^n + d_3 u_{k-2}^n \\ &\qquad + d_4 u_k^{n+1} + d_5 u_k^{n-1} + d_6 \mathcal{F}_k^n\Big\}, \end{aligned} \quad (24)$$

where $\theta = (\rho_u X_u)/(2T^2)$. Equation (6) can be used to replace $(u_k^{n+1}, u_k^n, u_k^{n-1})$ with $(v_{l,m}^{n+1}, v_{l,m}^n, v_{l,m}^{n-1})$. Assuming now that there are no further contributions to the force density term in (21), we substitute $\mathcal{F}_{l,m} = F_c/(X_v^2)$, which yields the final update equation at the connection point ($l = x_c/X_v$, $m = y_c/X_v$):

$$\begin{aligned} v_{l,m}^{n+1} &= g_1 v_{l,m}^n \\ &+ g_2(v_{l,m+1}^n + v_{l,m-1}^n + v_{l+1,m}^n + v_{l-1,m}^n) \\ &+ g_3(v_{l+1,m+1}^n + v_{l+1,m-1}^n + v_{l-1,m+1}^n + v_{l-1,m-1}^n) \\ &+ g_4(v_{l,m+2}^n + v_{l,m-2}^n + v_{l+2,m}^n + v_{l-2,m}^n) \\ &+ g_5(v_{l+1,m+2}^n + v_{l+1,m-2}^n + v_{l-1,m+2}^n + v_{l-1,m-2}^n + \\ &\ldots \quad v_{l+2,m+1}^n + v_{l+2,m-1}^n + v_{l-2,m+1}^n + v_{l-2,m-1}^n) \\ &+ g_6(v_{l+2,m+2}^n + v_{l+2,m-2}^n + v_{l-2,m+2}^n + v_{l-2,m-2}^n) \\ &+ g_7 v_{l,m}^{n-1} \\ &+ g_8(v_{l+1,m}^{n-1} + v_{l-1,m}^{n-1} + v_{l,m+1}^{n-1} + v_{l,m-1}^{n-1}) \\ &+ g_9(v_{l+1,m+1}^{n-1} + v_{l+1,m-1}^{n-1} + v_{l-1,m+1}^{n-1} + v_{l-1,m-1}^{n-1}) \\ &+ g_{10} u_{k-1}^n \\ &+ g_{11} u_{k-2}^n \\ &+ g_{12} \mathcal{F}_k^n. \end{aligned} \quad (25)$$

As will be explained in section 5.1, we also consider a string (displacement denoted with u) coupled with one of its ends to another string (displacement denoted with v). The connection point update equation can be derived in a similar fashion, leading to

$$\begin{aligned} v_l^{n+1} &= g_1\left(v_{l+2}^n + v_{l-2}^n\right) + g_2\left(v_{l+1}^n + v_{l-1}^n\right) + g_3 v_l^n + g_4 v_l^{n-1} \\ &+ g_5\left(v_{l+1}^{n-1} + v_{l-1}^{n-1}\right) + g_6 u_{k-1}^n + g_7 u_{k-2}^n + g_8 \mathcal{F}_k^n. \end{aligned} \quad (26)$$

Note that $\mathcal{F}_k^n$ in equations (25) and (26) denotes a possible external force density applied on the string at the connection point.

4. FD-MODAL FORMULATION

4.1. Projection onto a Modal Basis

The FD model of the string and plate can be formulated in matrix form. As an example, consider an ideal string (no stiffness or losses), fixed at both ends, with its displacement denoted by $v(x,t)$. The difference equation (14) then reduces to

$$v_l^{n+1} = (v_{l+1}^n + v_{l-1}^n) - v_l^{n-1} + \rho_v^{-1} T^2 \mathcal{F}_l^n, \qquad (27)$$

and the complete FD formulation can then be written in matrix form as follows

$$\mathbf{v}^{n+1} = \mathbf{A}\mathbf{v}^n - \mathbf{v}^{n-1} + \rho_v^{-1} T^2 \mathbf{f}, \qquad (28)$$

where $\mathbf{A}$ is tridiagonal matrix, and $\mathbf{v}^n$ and $\mathbf{f}^n$ are vectors holding the displacement and force density values at the $(M-1)$ interior points for a string discretised into M segments (i.e. excluding the boundary points which are held at zero). Projection onto a modal basis is performed by diagonalising this system of equations, giving

$$\mathbf{\Phi}^{n+1} = \underbrace{\mathbf{G}^{-1}\mathbf{A}\mathbf{G}}_{\mathbf{D}}\mathbf{\Phi}^n - \mathbf{\Phi}^{n-1} + \rho_v^{-1} T^2 \underbrace{\mathbf{G}^{-1}\mathbf{f}^n}_{\bar{\mathbf{f}}^n}. \qquad (29)$$

where the matrix $\mathbf{G}$ holds the the eigenvectors of $\mathbf{A}$, and the matrix $\mathbf{D}$ is diagonal, containing the eigenvalues of $\mathbf{A}$. Equation (29) shows that the system can be computed by updating a set of uncoupled equations, each of which represents a second order oscillator, similar to those employed in Modal Synthesis [14]. The state of each oscillator is updated with

$$\phi_i^{n+1} = b_{1,i}\bar{f}_i^n - a_{1,i}\phi_i^n - \phi_i^{n-1}, \qquad (30)$$

where $b_{1,i} = T^2/\rho_v$ and where $a_{1,i}$ is the ith diagonal element of $-\mathbf{D}$. The latter can be related to the frequency of the second-order oscillator with $a_{1,i} = -2\cos(\omega_i T)$. The displacements can be calculated directly from the oscillator states with

$$\mathbf{v}^{n+1} = \mathbf{G}\phi^{n+1}, \qquad (31)$$

and the force density input signals are calculated with

$$\bar{\mathbf{f}}^n = \mathbf{G}^{-1}\mathbf{f}^n. \qquad (32)$$

It is readily seen that if we multiply $\mathbf{G}$ with a scalar of the dimension of one over length (m^{-1}), $\bar{\mathbf{f}}^n$ becomes a force term rather than a force density term, and that this alteration has no effect on the output, since it will be cancelled out with (31). Put in another way, we may replace $\mathbf{f}^n$ with an actual force term $\mathbf{F}^n$ as long as we also scale the output by an appropriate normalisation factor η of the dimension (m^{-1}). For 2D objects, this normalisation factor will be of the dimension (m^{-2}) (See section 4.4).

4.2. Comparison to the Functional Transformation Method

The Functional Transformation Method (FTM) is a physical modelling paradigm that directly translates the underlying differential equations into a structure for calculating the displacement at any point along a vibrating object as a weighted set of second-order oscillator[3] states [4, 5]. The main difference with the FD method is that the FTM does not involve spatial discretisation, and that it uses the impulse invariant transform to obtain a discrete-time model for each modal oscillator. Its main advantage is that no numerical dispersion or attenuation is introduced; the main limitation is that closed-form expressions for the final coefficients of the model can only be found for idealised cases; in particular, it cannot easily handle irregular domains [5].

Since for an ideal string, the FD method also does not introduce any numerical dispersion or attenuation, a direct comparison with the FTM is particularly illuminating for this case. For an ideal string, the FTM can be seen to effectively update the oscillators states according to (30), using the coefficients (see [4]):

$$b_{1,i} = \frac{T\sin(\omega_i T)}{\rho_v \omega_i}, \qquad (33)$$

$$a_{1,i} = -2\cos(\omega_i T). \qquad (34)$$

In other words, only the $b_{1,i}$ coefficients are different in comparison to the diagonalised FD method. This difference vanishes when one calculates the velocity of both models rather than the displacement. In the diagonalised FD model, one then applies a centered operator to the output of each oscillator, which can also be interpreted as multiplying the $b_{1,i}$ with $(z - z^{-1})/(2T)$, where $z = e^{j\omega T}$. From the fact that for any single oscillator, we have only one frequency to consider $\omega = \omega_i$, we can thus write the $b'_{1,i}$ coefficient for calculating the velocity output of mode i as

$$b'_{1,i} = \frac{T^2(e^{j\omega_i T} - e^{j\omega_i T})}{2\rho_v T} = \frac{T\sin(\omega_i T)}{\rho_v}. \qquad (35)$$

For the FTM, we can directly differentiate with respect to time by multiplying (33) with ω_i, leading exactly to (35), which suggests mathematical equivalence of the two paradigms for the ideal lossless string when observing velocity output.

4.3. Adding Modal Damping

While it is straightforward to include damping from the start for an FD model, in the case of projection on a modal basis, the damping may also be imposed after diagonalisation (thus avoiding numerical attenuation). In addition, we now consider an excitation force (F) at a single position on the body, and apply this directly to the second-order oscillators, incorporating the modal excitation weighting into the $b_{1,i}$ coefficients. These adjustments lead to the modal oscillator update equations of the form

$$\phi_i^{n+1} = b_{1,i}F^n - a_{1,i}\phi_i^n - a_{2,i}\phi_i^{n-1}, \qquad (36)$$

where

$$b_{1,i} = \frac{V_i T^2 e^{-\alpha_i T}}{\rho_v}, \qquad (37)$$

$$a_{1,i} = -2e^{-\alpha_i T}\cos(\omega_i T), \quad a_{2,i} = e^{-2\alpha_i T}. \qquad (38)$$

where α_i and k_i denote the decay rate and wave number of mode i, respectively, and V_i represents the modal excitation weight that depends on the excitation position. It can be seen that - for simply supported boundary conditions and assuming zero initial conditions - the FTM effectively uses the same formulation [4], be it that equation (37) is replaced by

$$b_{1,i} = \frac{V_i T e^{-\alpha_i T}\sin(\omega_i T)}{\rho_v \omega_i}, \qquad (39)$$

although the weightings V_i (these are called "transformation kernels" in [4, 5]) are not included in the coefficients there, but applied separately.

[3] In some scenarios, complex first-order filters are used instead [5].

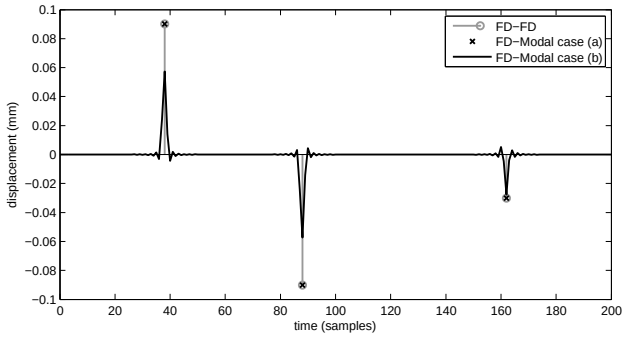

Figure 2: *Displacement of the second string at 1/5 of its length when exciting an ideal string-string system at the connection point.*

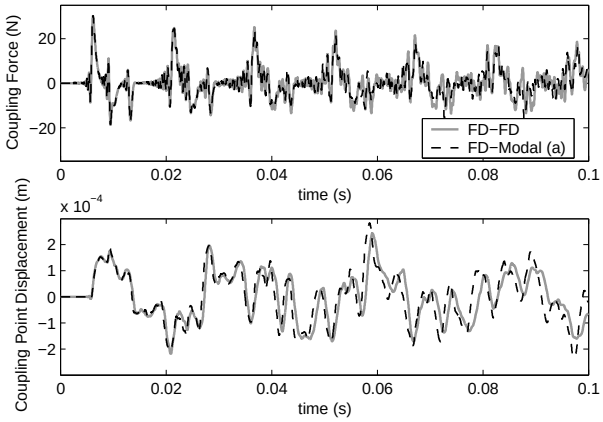

Figure 3: *Force (top) and displacement (bottom) at the connection point, for the plate-string system excited with a hammer-string model.*

4.4. Modal Representation of a Simply Supported Plate

In order to formulate a plate in modal form, the diagonalisation of an FD model of a 2D, stiff and lossy system is considerably more complex than for a simple ideal string, but in principle it can be used as a basis. Given that the numerical dispersion is quite large for explicit FD models, it is a good idea then to start instead from an implicit FD formulation, which allows reducing such errors significantly.

For idealised resonators, such as a rectangular plate with simply supported edges, one may of course derive the modal parameters (frequency, damping, weights) in an analyic fashion (for example using the FTM). This is what is used for the example applications in this study, with one alteration, namely that the $b_{1,i}$ coefficients are set as predicted by the FD formulation, i.e. as in (37). As will be seen in section 5.1, this ensures that when the plate is coupled to the string, certain FD features are preserved.

Taking such an analytical approach, the transverse displacement of the plate at any point (x, y) can be calculated in modal form with:

$$v^{n+1} = \eta \sum_{i=1}^{N_m} W_i \ \phi_i^{n+1}, \tag{40}$$

where $\eta = 4/(L_x L_y)$ is the normalisation factor, N_m is the number of modes taken into account and where W_i are the modal 'pick-up' weights, that depend on observation position. For lossy plates, the modal frequency and decay rate can be defined for mode (m, n) with wave number k_{mn} as

$$\omega_{mn} = \sqrt{\kappa_v^2 k_{mn}^4 - \alpha_{mn}^2}, \tag{41}$$

$$\alpha_{mn} = b_{1v} + b_{2v} k_{mn}^2. \tag{42}$$

The associated modal excitation and pick-up weights for the relative excitation position (x_e, y_e) and relative pick-up position (x_p, y_p) are [11]

$$V_{mn} = \sin(m\pi x_e/L_x)\sin(n\pi y_e/L_y), \tag{43}$$

$$W_{mn} = \sin(m\pi x_p/L_x)\sin(n\pi y_p/L_y). \tag{44}$$

The values of ω_{mn}, α_{mn}, V_{mn} and W_{mn} that correspond to frequencies below Nyquist can be collected and stored in long flat vectors, thus forming the modal data ω_i, α_i, V_i and W_i that can be directly applied in the modal formulation of the plate.

4.5. Updating the Connection Point

In this section, the coupling of the FD difference string with a modal resonant body is presented. Given the generality of the modal representation, the resonant body could be any linearly vibrating system. In this scenario, the only force applied to the body is that exerted by the string at the connection point, and we need to calculate the displacement (v_c) at that same point. In other words, the plate (or other resonant body) is locally characterised by a transfer function. In order to derive a computable update formula, first equation (36) is substituted into equation (40), which yields

$$v_c^{n+1} = \eta \sum_{i=1}^{N_M} W_i \left\{ b_{1,i} F_c^n - a_{1,i}\phi_i^n - a_{2,i}\phi_i^{n-1} \right\}, \tag{45}$$

or

$$v_c^{n+1} = F_c^n \underbrace{\eta \sum_{i=1}^{N_m} W_i b_{1,i}}_{\beta} - \underbrace{\eta \sum_{i=1}^{N_m} B_i \left(a_{1,i}\phi_i^n + a_{2,i}\phi_i^{n-1}\right)}_{H^n}, \tag{46}$$

or

$$v_c^{n+1} = \beta F_c^n - H^n. \tag{47}$$

At the connection point, the force is still defined by equation (24). This force term can be substituted into (47), which yields:

$$v_c^{n+1} = g_1 v_c^n + g_2 u_{k-1}^n + g_3 u_{k-2}^n + g_4 v_c^{n-1} + g_5 \mathcal{F}_k^n + g_6 H^n. \tag{48}$$

5. RESULTS

5.1. Model Equivalence for String-String Coupling

In order to test the validity of the modal formulation within an FD modelling framework, simulations of an ideal string coupled with one end to the center of another ideal string (of equal tension) were carried out; the first string was fixed at its left end, and the second string (acting as the 'resonant body') was fixed at both ends. This

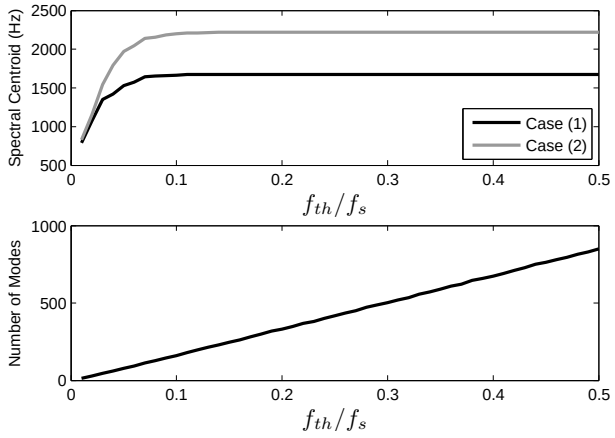

Figure 4: *Spectral centroid (top) and number of modes (bottom) as a function of normalised threshold frequency for the case of a hammered string coupled to a plate.*

coupling of two transversely vibrating strings is of course rather artificial and unlike any real string instrument; it is used here merely to demonstrate certain system features.

Three different models were used: the FD-FD model, the FD-Modal (a) model that uses equation (37) for the $b_{1,i}$ coefficients, and the FD-Modal (b) model that uses equation (39) for the $b_{1,i}$ coefficients. The comparison between these three cases is useful, since the FD-FD model exhibits no numerical dispersion or attenuation for the ideal string provided that the Courant number is chosen exactly at the stability bound. Hence any deviations between these models should be small, and shed further light on the effects of the choice for the $b_{1,i}$ coefficients.

In the simulation, a perfect wave impulse was generated at the connection point, and the displacement of the second string at 1/5 from one of its ends was recorded. Figure (2) shows the resulting displacement signals for the three models. It can be seen that the FD-Modal (a) model gives exactly the same response as the FD-FD model, thus validating the use of equation (37). The FD-Modal (b) model gives a similar response, but with the noticable difference that the original pulse shape applied is not exactly preserved and takes on a bandlimited nature. Note that this discrepancy does not indicate any deficiency of either paradigm, but merely highlights that since FD models using force and displacement as their variables (rather than force and velocity), the FTM needs to be adapted in order to interface directly to an FD model.

5.2. Comparison for String-Plate Coupling

Moving on now to a somewhat more realistic scenario, the resonant body has been upgraded to a thin, lossy plate of $0.4\text{m} \times 0.4\text{m}$, and the string has been made stiff and lossy. Moreover, the string is now excited with a hammer-string interaction model [15], taking all the string parameters as those for a piano C2 string from [10]. For the plate we used $\kappa_v = 2\text{m}^2\text{s}^{-1}$, $b_{v1} = 1s^{-1}$, $b_{v2} = 0.01\text{m}^2\text{s}^{-1}$, and $\rho_v = 10\text{kg m}^{-2}$. Figure (3) shows the force and displacement at the connection point, as calculated with the FD-FD and FD-Modal (a) model. As expected, the two models now show some small discrepancy (due to numerical dispersion in the FD-FD model), but the overall match is still quite close. Interestingly, the computation time in MATLAB for the FD Modal model is in this case about half of that required for the FD-FD model. This can be explained by the fact that the FD-FD model, if translated directly into modal form (as in section 4.1), would result in about twice the number of modes. The explicit FD-FD system is thus larger in order due to spatial discretisation.

Table 1: *Spectral centroid analysis. N_m is the number of modes, f_{sc} is the spectral centroid, Δf_{sc} is the difference with f_{sc} for $f_{th} = 0.5$, and f_1 is the fundamental frequency.*

		Case (1): $b_{v1} = 3, b_{v2} = 0.01$		Case (2): $b_{v1} = 10, b_{v2} = 0$	
f_{th}/f_s	N_m	f_{sc} (Hz)	$\Delta f_{sc}/f_1$	f_{sc} (Hz)	$\Delta f_{sc}/f_1$
0.5	849	1675	0	2222	0
0.12	197	1673	0.038	2212	0.15
0.1	160	1664	0.17	299	0.34
0.05	77	1530	2.23	1973	3.8

5.3. Reducing Computational Complexity

A key advantage of the modal formulation is that the number of modes that is included is adjustable, which allows to scale the computational complexity. Normally, one would include all (not overdamped) modes with frequencies lower than Nyquist, but sounds that are perceptually close can be generated with a lower number of modes. For example, one could remove all modes with decay rates higher than a certain threshold, or include frequencies up to a lower bound than Nyquist (the latter is used in this study). In practice, both amount to reducing the bandwidth.

The FD-FD model can also be scaled, by simply lowering the sample rate, which also reduces the computational load along with the model bandwidth. However because of numerical dispersion, the scaling down has in this case detrimental effects on the modes within the remaining model bandwidth, whereas no such effects occur with scaling down the FD-Modal formulation by mode-culling.

From a sound synthesis perspective, it is interesting then to know how many modes may be removed before the FD-Modal model starts to sounds different in comparison to the full-bandwidth version. In order to investigate this, the FD-Modal simulation was run for a decreasing set of bandwidths, i.e. gradually lowering the threshold frequency f_{th} above which no modes are included. To get a first approximation of how the timbre of the resulting sound changes with f_{th}, the spectral centroid was calculated. Figure 4 shows, for two different sets of plate damping parameters, how the spectral centroid and the number of modes (that can be considered as a metric for computational complexity) vary with f_{th}. Table 1 lists the devations from $f_{th} = 0.5$ divided by the fundamental frequency of the for selected values of f_{th}/f_s. The results indicate that when lowering f_{th}, the decrease in spectral centroid remains smaller than the just noticable difference - which in this case is about 10 Hz (15% of the fundamental [16]) - as long as f_{th} is higher than about $0.12 f_s$. This suggests that one may use about one fourth of the modes without a noticable change in the sound, which is in alignment with what was experienced in informal lis-

tening tests. It is difficult though to make general, precise conclusions regarding the allowable amount of disregarded modes, since such results depend on many factors, including the sample rate, the damping parameters, and the character of the excitation signal. In addition, the spectral centroid is just a single timbre indicator. The advantage of scalability is evident though from this example.

5.4. Sound Examples

The FD-Modal model can be employed to generate a wide range of sonorities. For example, it is straightforward to connect multiple strings to a plate, and simulate classical phenomena such as two-stage decay, beatings and sympathetic vibrations. One of our more adventurous experiments centered around variation of the plate mass density, which can be used to change a piano-like tone to a percussive sounding tone that is characterised dominantly by the plate resonances. In another experiment, we explored on-line parameter changes that are difficult if not impossible with real-life instruments, such as slowly changing the connection position on the plate. A selection of sound examples can be found and explored on www.sarc.qub.ac.uk/∼mvanwalstijn/DAFx09/.

6. CONCLUDING REMARKS

Novel numerical formulations for simulation of a string rigidly coupled to a resonant body have been proposed. A full finite difference formulation of a string coupled to a plate (FD-FD model) has been presented, and a second model (FD-Modal) was derived in which the plate is represented in modal form. The key part of both models is the connection point update formula that implements the coupling conditions. For the FD-Modal formulation, a slight coefficient adjustment in comparison to previously developed modal representations is made in order to preserve the finite difference character of the simulation. The main advantage of the FD-Modal formulation is that it allows direct scaling of computational complexity without introducing artefacts to the remaining model bandwidth, thus making it attractive for real-time applications. In our examples, the computational complexity of the plate model was reduced by as much as 80% without noticable changes to the sound; further reductions can be made by multi-rate implementation methods.

Because of the generality of the modal basis, the FD-Modal model may be used for simulation of a string coupled to an arbitrary linearly behaving resonant body. For resonant bodies that can be modelled by analytic modal decomposition, the FD-Modal model can be regarded as an FD model without the numerical artefacts of the body part of the system. For all other cases, the modal data has to be either measured or pre-calculated by diagonalising numerical methods, such as the FD method or the Finite Element (FE) method, possibly at a higher sample rate in order to reduce numerical dispersion. The FE method would be particularly appropriate in case of dealing with real instument bodies, since it is particularly suited to modelling objects with complicated geometries [14]. Other aspects of interest for future work include extension to geometric nonlinearities and modelling bridge elements, both of which require to reformulate the coupling conditions in order to model interaction in more than one dimension.

7. REFERENCES

[1] L. Sujbert B. Bank, "Generation of longitudinal vibrations in piano strings: From physics to sound synthesis," *Journal of the Acoustical Society of America*, vol. 117, no. 4, pp. 2268–2278, April 2005.

[2] S. Bilbao, "Conservative numerical methods for nonlinear strings," *The Journal of the Acoustical Society of America*, vol. 118, no. 5, pp. 3316–3327, 2005.

[3] M. Karjalainen J. Pakarinen, V. Valimaki, "Physics-based methods for modeling nonlinear vibrating strings," *Acta Acustica united with Acustica*, vol. 91, pp. 312 – 325, 2005.

[4] Rudolf Rabenstein and Lutz Trautmann, "Digital sound synthesis of string instruments with the functional transformation method," *Signal Processing*, vol. 83, no. 8, pp. 1673 – 1688, 2003.

[5] L. Trautmann and R. Rabenstein, *Digital Sound Synthesis by Physical Modelling Using the Functional Transformation Method*, Kluwer Academic / Plenum Publishers, 2003.

[6] A. Taflove and S. C. Hagness, *Computational Electrodynamics: The Finite Difference Time-Domain method*, Artech House, third edition, 2005.

[7] S. Petrausch and R. Rabenstein, "Sound synthesis by physical modelling using the functional transformation method: Efficient implementation with polyphase-filterbanks," *Proc. of the 6th Int. Conference on Digital Audio Effects (DAFx-03)*, 2003.

[8] M. Karjalainen and C. Erkut, "Digital waveguides versus finite difference structures: Equivalence and mixed modeling," *EURASIP J. Appl. Signal Process.*, vol. 7, pp. 987–989, 2004.

[9] R. Rabenstein, S. Petrausch, A. Sarti, G. De Sanctis, C. Erkut, and M. Karjalainen, "Block-based physical modeling for digital sound synthesis," *IEEE Signal Processing Magazine*, vol. 24, no. 2, pp. 42–54, 2007.

[10] J. Bensa, S. Bilbao, R. Kronland-Martinet, and J. O. Smith III, "The simulation of piano string vibration: From physical models to finite difference schemes and digital waveguides," *Journal of the Acoustical Society of America*, vol. 114, no. 2, pp. 1095–1107, August 2003.

[11] N. H. Fletcher and T. D. Rossing, *The Physics of Musical Instruments*, Springer, second edition, 1998.

[12] S. Bilbao, L. Savioja, and J.O. Smith, "Parameterized finite difference schemes for plates: Stability, the reduction of directional dispersion and frequency warping," *Audio, Speech, and Language Processing, IEEE Transactions on*, vol. 15, no. 4, pp. 1488 – 1495, May 2007.

[13] M. van Walstijn and K. Kowalczyk, "On the numerical solution of the 2d wave equation with compact FDTD schemes," *Proc. of the 11th Int. Conference on Digital Audio Effects (DAFx-08)*, 2008.

[14] Cynthia Bruyns, "Modal synthesis for arbitrarily shaped objects," *Comput. Music J.*, vol. 30, no. 3, pp. 22–37, 2006.

[15] A. Chaigne and A. Askenfelt, "Numerical simulations of piano strings I. A physical model for a struck string using finite difference methods," *Journal of the Acoustical Society of America*, vol. 95, no. 2, pp. 1112–1118, February 1994.

[16] R. A. Kendall and E. C. Carterette, "Difference threshold for timbre related to spectral centroid," *Proceedings of the Fourth International Conference on Music Perception and Cognition*, 1996.

8. APPENDIX

The appendix provides the coefficient formulae for all difference equations presented in the paper.

8.1. The String

The coefficients of equation (14) are:

$$\begin{aligned} a_{1u} &= \big(2 - 2\lambda_u^2 - 6\mu_u^2 - 2\nu_{2u}\big)/\big(1+\nu_{1u}\big), \\ a_{2u} &= \big(\lambda_u^2 + 4\mu_u^2 + \nu_{2u}\big)/\big(1+\nu_{1u}\big), \\ a_{3u} &= \big(-\mu_u^2\big)/\big(1+\nu_{1u}\big), \\ a_{4u} &= \big(-1+\nu_{1u}+2\nu_u\big)/\big(1+\nu_{1u}\big), \\ a_{5u} &= \big(-\nu_{2u}\big)/\big(1+\nu_{1u}\big), \\ a_{6u} &= \big(T^2\rho_u^{-1}\big)/\big(1+\nu_{1u}\big), \end{aligned} \tag{49}$$

where

$$\mu_u = \frac{\kappa_u T}{X_u^2}, \quad \nu_{1u} = b_{1u}T, \quad \nu_{2u} = \frac{2b_{2u}T}{X_u^2} \quad \lambda_u = \frac{cT}{X_u}. \tag{50}$$

8.2. The Plate

The coefficients of equation (21) are:

$$\begin{aligned} a_{1v} &= \big(2 - (9\alpha^2 + 6\alpha + 5)\mu^2 - 2\nu_{2v}(1+\alpha)\big)/\big(1+\nu_{1v}\big), \\ a_{2v} &= \big((6\alpha^2 + 2\alpha)\mu^2 + \nu_{2v}\alpha\big)/\big(1+\nu_{1v}\big), \\ a_{3v} &= \big((-4\alpha^2 + 2)\mu^2 + 0.5\nu_{2v}(1-\alpha)\big)/\big(1+\nu_{1v}\big), \\ a_{4v} &= \big((-1.5\alpha^2 + \alpha - 0.5)\mu^2\big)/\big(1+\nu_{1v}\big), \\ a_{5v} &= \big((\alpha^2 - \alpha)\mu^2\big)/\big(1+\nu_{1v}\big), \\ a_{6v} &= \big((-0.25\alpha^2 + 0.5\alpha - 0.25)\mu^2\big)/\big(1+\nu_{1v}\big), \\ a_{7v} &= \big((\nu_{1v} - 1) + 2\nu_{2v}(1+\alpha)\big)/\big(1+\nu_{1v}\big), \\ a_{8v} &= \big(-\nu_{2v}\alpha\big)/\big(1+\nu_{1v}\big), \\ a_{9v} &= \big(-0.5\nu_{2v}(1-\alpha)\big)/\big(1+\nu_{1v}\big), \\ a_{10v} &= \big(T^2/\rho_v\big)/\big(1+\nu_{1v}\big), \end{aligned} \tag{51}$$

where

$$\mu_v = \frac{\kappa_v T}{X_v^2}, \quad \nu_{1v} = b_{1v}T, \quad \nu_{2v} = \frac{2b_{2v}T}{X_v^2}. \tag{52}$$

8.3. The String Force

The coefficients of equation (24) are:

$$\begin{aligned} d_1 &= 2 - 2\mu_u^2 - 2\lambda_u^2, \\ d_2 &= 2(\lambda_u^2 + 2\mu_u^2), \\ d_3 &= -2\mu_u^2, \\ d_4 &= -1 - \nu_{1u}, \\ d_5 &= -1 + \nu_{1u}, \\ d_6 &= \rho_u^{-1}T^2. \end{aligned} \tag{53}$$

8.4. Connection Point in the String-Plate System (FD-FD)

The coefficients of equation (25) are:

$$\begin{aligned} g_1 &= \big(a_{1v} + \xi d_1\big)/\big(1 - \xi d_4\big) \\ g_2 &= \big(a_{2v}\big)/\big(1 - \xi d_4\big), \\ g_3 &= \big(a_{3v}\big)/\big(1 - \xi d_4\big), \\ g_4 &= \big(a_{4v}\big)/\big(1 - \xi d_4\big), \\ g_5 &= \big(a_{5v}\big)/\big(1 - \xi d_4\big), \\ g_6 &= \big(a_{6v}\big)/\big(1 - \xi d_4\big), \\ g_7 &= \big(a_{7v} + \xi d_5\big)/\big(1 - \xi d_4\big), \\ g_8 &= \big(a_{8v}\big)/\big(1 - \xi d_4\big), \\ g_9 &= \big(a_{9v}\big)/\big(1 - \xi d_4\big), \\ g_{10} &= \big(\xi d_2\big)/\big(1 - \xi d_4\big), \\ g_{11} &= \big(\xi d_3\big)/\big(1 - \xi d_4\big), \\ g_{12} &= \big(\xi d_6\big)/\big(1 - \xi d_4\big), \end{aligned} \tag{54}$$

where ξ is the coupling parameter

$$\xi = \frac{\theta\, a_{10v}}{X_v^2} = \frac{1}{2(1+\nu_{1v})}\frac{\rho_u X_u}{\rho_v X_v^2}. \tag{55}$$

8.5. Connection Point in the String-String System (FD-FD)

The coefficients of equation (26) are:

$$\begin{aligned} g_1 &= \big(a_{1v}\big)/\big(1 + \xi d_4\big), \\ g_2 &= \big(a_{2v}\big)/\big(1 - \xi d_4\big), \\ g_3 &= \big(a_{3v} + \xi d_1\big)/\big(1 - \xi d_4\big), \\ g_4 &= \big(a_{4v} + \xi d_5\big)/\big(1 - \xi d_4\big), \\ g_5 &= \big(a_{5v}\big)/\big(1 - \xi d_4\big), \\ g_6 &= \big(\xi d_2\big)/\big(1 - \xi d_4\big), \\ g_7 &= \big(\xi d_3\big)/\big(1 - \xi d_4\big), \\ g_8 &= \big(\xi d_6\big)/\big(1 - \xi d_4\big), \end{aligned} \tag{56}$$

where the a_{iv} coefficients are now calculated as in (49), and where

$$\xi = \frac{1}{2(1+\nu_{1v})}\frac{\rho_u X_u}{\rho_v X_v}. \tag{57}$$

8.6. Connection Point (FD-Modal)

The coefficients of equation (48) are:

$$\begin{aligned} g_1 &= \big(\beta\theta d_1\big)/\big(1 - \beta\theta d_4\big), \\ g_2 &= \big(\beta\theta d_2\big)/\big(1 - \beta\theta d_4\big), \\ g_3 &= \big(\beta\theta d_3\big)/\big(1 - \beta\theta d_4\big), \\ g_4 &= \big(\beta\theta d_5\big)/\big(1 - \beta\theta d_4\big), \\ g_5 &= \big(\beta\theta d_6\big)/\big(1 - \beta\theta d_4\big), \\ g_6 &= \big(-1\big)/\big(1 - \beta\theta d_4\big), \end{aligned} \tag{58}$$

where $\theta = (\rho_u X_u)/(2T^2)$.